

Accepted manuscript for Journal of Natural Gas Science and Engineering

## Innovative method to prepare a stable emulsion liquid membrane for high CO<sub>2</sub> absorption and its performance evaluation for a natural gas feed in a rotating disk contactor

Inamullah Bhatti<sup>a</sup>, Khadija Qureshi<sup>a</sup>, Khairul Sozana Nor Kamarudin<sup>b</sup>, Aqeel Ahmed Bazmi<sup>c</sup>, Abdul Waheed Bhutto<sup>a, d</sup>, Faizan Ahmad<sup>e, \*</sup>, Moonyong Lee<sup>f</sup>

<sup>a</sup> Department of Chemical Engineering, Mehran University of Engineering and Technology, Jamshoro, Sindh, Pakistan

<sup>b</sup> Chemical Engineering Department, Universiti Teknologi Malaysia, 81310 Skudai, Johor, Malaysia

<sup>c</sup> Process and Energy Systems Engineering Center-PRESTIGE, Department of Chemical Engineering, COMSATS Institute of Information Technology, Lahore, Pakistan.

<sup>d</sup> Department of Chemical Engineering, Dawood University of Engineering and Technology, Karachi, Pakistan

<sup>e</sup> School of Science and Engineering, Teesside University, Middlesbrough, United Kingdom

<sup>f</sup> Process Systems Design and Control Laboratory, Yeungnam University, Gyeongsan, Republic of Korea

\*Authors to whom correspondence should be addressed;

### **Faizan Ahmad**

School of Science and Engineering, Teesside University, Middlesbrough, Tees Valley, TS1 3BA, United Kingdom

Telephone: 0044-1642-342294 E-mail: [f.ahmad@tees.ac.uk](mailto:f.ahmad@tees.ac.uk)

Alternative e-mail: [faizan615@gmail.com](mailto:faizan615@gmail.com)

## **Abstract**

This paper presents a new method to prepare a stable emulsion liquid membrane (ELM) for high CO<sub>2</sub> absorption in a natural gas feed. The ELM prepared using this new method was characterized by determining the effects of the concentration of the ELM constituents, emulsification time, and speed on the emulsion droplet size (EDS) and stability. This was followed by a parametric study of the process parameters for CO<sub>2</sub> separation from natural gas in a rotating disk contactor (RDC)-based setup to evaluate the performance of a stable ELM. The results suggest that the retention time of the stable ELM in a rotating disc contactor increases with increasing amount of absorbed CO<sub>2</sub>. The results support the fundamental development of the ELM process to achieve a high overall separation efficiency of CO<sub>2</sub> removal from natural gas with a relatively small contact time. This is the first parametric study of CO<sub>2</sub> absorption from a gas stream in ELM using a RDC as the contacting equipment.

**Keywords:** Emulsion liquid membrane; CO<sub>2</sub> absorption; rotating disc contactor; natural gas; separation processes

## **1. Introduction and Background**

Natural gas extracted from wells often contains 10 – 20 mol. (20–40 wt. %) % CO<sub>2</sub> [1]. A number of methods exist for the capture of CO<sub>2</sub> from gases. These methods include chemical absorption, physical absorption, membrane separation, adsorption, and cryogenic separation [2, 3]. Traditionally, amine absorption is used to remove CO<sub>2</sub> from natural gas and hydrogen [4]. The mass transfer limitations encountered in the conventional absorption process have prompted a search for alternative methods. Membrane processes are major competitors with conventional

amine absorption technology for CO<sub>2</sub> capture from the natural gas separation process [5]. Emulsion liquid membrane (ELM) processes allow very high mass transfer rates due to the large surface area within the emulsion globules and internal droplets [6]. The other remarkable features of membrane technology include low energy consumption, low capital investment, mild condition, and the ease of combination with other separation processes [7, 8]. This has led to massive research efforts into membrane-based gas separation technology [9].

Li invented the ELM separation technique in 1968 [10], which is based on selective permeation through a liquid surfactant membrane. An ELM is a three-phase dispersion system, where a primary emulsion is dispersed in a continuous effluent phase, which is the phase to be treated [11]. The dispersed phase of the emulsion drops consists of low viscosity organic diluents, a surfactant to stabilize the emulsion and sometimes a carrier. Liquid membranes or a liquid film separates two phases from each other. The phenomena of micro size droplets of an immiscible liquid dispersed into a continuous liquid phase have been described with a qualitative explanation by several researchers [12, 13]. Linek and Benes [14] examined the absorption of gas into an oil-in-water (o/w) or water-in-oil (w/o) emulsion and observed that the mass transfer coefficient is unaffected by the oil content in the o/w type of emulsion, whereas it increased in proportion to the w/o emulsion with the volume fraction of oil.

**Fig.1** presents the structure of the ELM system. The emulsions are produced by shearing two immiscible liquids, which provides the energy necessary to reach a metastable state through the fragmentation of one phase into another. The persistence of such dispersions is generally assured by the presence of surface active species (surfactant), which are known to cover the interfaces and are responsible for significantly delaying the coalescence of the droplets [15]. From their

preparation to their destruction, the emulsions reveal many kinds of both reversible and irreversible transitions. Irreversible phenomena lead to coarsening, which may originate from either coalescence or Ostwald ripening [15].

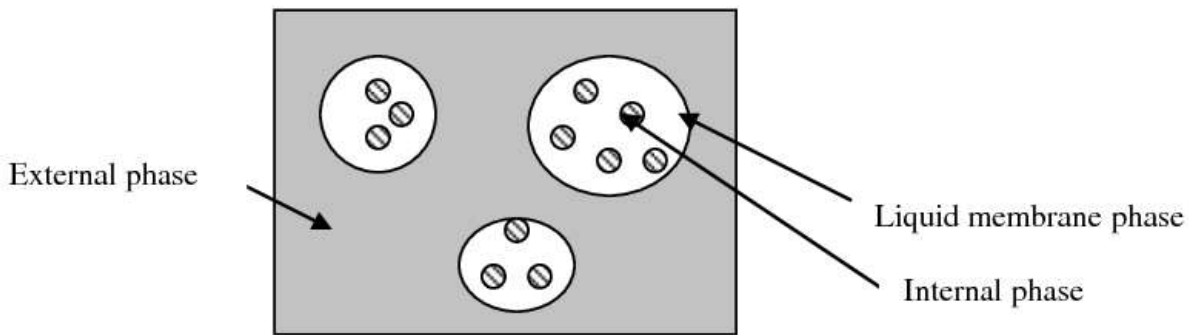


**Fig. 1.** Structure of ELM system

Separation takes place in the liquid membranes, similar to the solid film, due to the solubility and diffusivity difference in the liquid film. The carrier in the membrane forms a complex with a specific solute and the carrier becomes mobile when it is dissolved in the liquid. On the other hand, the carrier in the solid membranes is bound chemically (covalently) or physically to the membrane surface. Understandably, the diffusivity in mobile carrier is much higher than in the fixed membrane. The absorption processes using ELM, where water-in-oil emulsions disperse in an aqueous phase are highly efficient in removing a variety of organic and inorganic materials in a range of applications [5]. Kaminski [16] discussed the pros and cons of EMS. Liquid membranes are highly selective and specific molecular detection is possible using the carriers for the transport mechanism. The reactive carrier species in the liquid membrane makes it highly selective compared to the other membranes.

Despite the advantages, ELM has not found widespread applications in industry because of the unsolved problems of the (i) stability and coalescence of emulsions and (ii) dissolution of membranes and substances they contain in the surrounding phases. The physical instability of emulsion globules is caused by fluid shear. The extraction process is also hindered by the emulsion breakup and the unwanted release of an internal receiving phase to the external contributing phase. This study reports a new method to prepare a stable ELM for high CO<sub>2</sub> absorption in the natural gas feed. A stable ELM requires an extractant capable of reacting with CO<sub>2</sub> at the gas liquid interface and diffusing easily, a stripping agent as a carrier and a surfactant for emulsion stability. The characterization of ELM prepared using the new method was followed by the parametric study of CO<sub>2</sub> separation from natural gas in RDC to evaluate its performance. This study extends the fundamental understanding of the ELM system to separate CO<sub>2</sub> from natural gas. The development in this area would lead to a decrease in cost and increase the separation efficiency of CO<sub>2</sub> from natural gas.

To evaluate the performance of the ELM prepared using the new method presented here, a RDC was chosen as the contactor equipment to conduct the parametric study of CO<sub>2</sub> separation from natural gas. RDC was selected because of their easy construction, high throughput, and low power consumption [17]. In the column-based operation, the liquid phase flows downward and gas phase flows upward, but with a very high contact surface area. The agitation provided by the discs breaks the disperse phase droplets, thereby increasing the interfacial area for mass transfer [18]. The mass transfer efficiency of commercial RDC is low, but the ELM process allows very high mass transfer rates due to the large surface area within the emulsion globules and internal droplets.

## 2. Experimental design

The block diagram in Fig. 2 summarizes the overall experimental work.

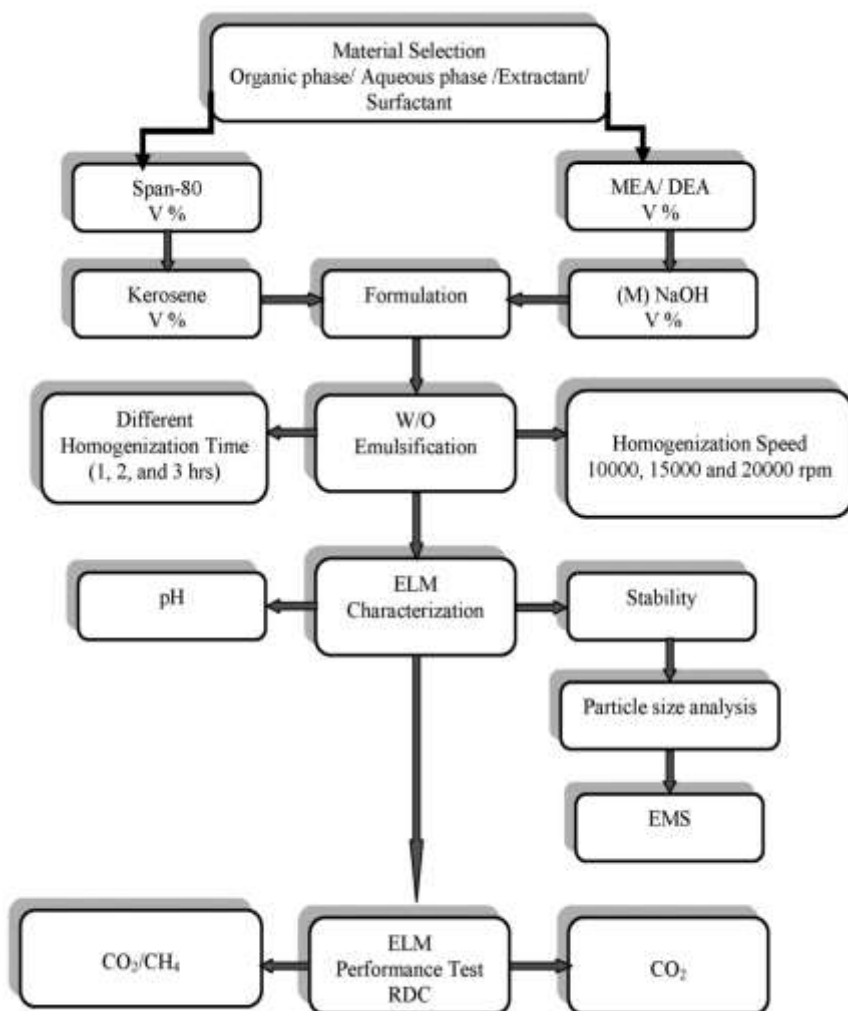


**Fig. 2.** Experimental Design

The experimental work in this study includes the selection of material and emulsifying equipment, suitable formulation of the emulsion constituents, and optimization of their formulation, followed by the formulation and characterization of a stable and effective emulsion.

Further experiments for CO<sub>2</sub> absorption by a stable ELM in RDC were conducted to determine the performance of the stable ELM under different operating parameters.

### **3. Preparation of a stable ELM**

The ELM was developed using the high-speed homogenization method. Both the organic phase and the aqueous phase were prepared separately and the aqueous phase was then dispersed in the organic phase to form a w/o ELM. This innovative process is simple in construction and provides high throughput with low power consumption.

#### **3.1. Aqueous phase**

The aqueous phase was prepared by dissolving the extractant in the NaOH solution. The required amount of aqueous solution was prepared and the extractant was then added. The resulting solution was heated and stirred for 15 minutes. The stirring speed and temperature of the heating plate was fixed to 700 rpm and 30°C, respectively.

#### **3.2. Organic phase**

The organic phase was composed of organic diluents and a surfactant. In this study, kerosene was used as the organic phase and triethylamine (TEA) was dissolved in the internal aqueous phase as the extractant. To increase the stability of the ELM, Span-80 ((sorbitan monooleate with a molecular weight of 428) was used as the surfactant. The organic phase was prepared by pouring the required volume of kerosene into the beaker followed by the addition of Span-80. The solution was heated and stirred for 15 minutes. The stirring speed and heating temperature were fixed to 700 rpm and 30°C, respectively.

### **3.3. Water oil emulsion**

The water oil emulsion (w/o) was prepared using kerosene as the membrane phase and an aqueous solution of NaOH as the dispersed phase. Different concentrations of TEA (2, 4 and 6 volume percent) were added to the aqueous phase act as an extractant. To avoid the high shear rate and non-Newtonian behavior of the emulsion, the ratio of the internal aqueous phase to the organic membrane phase was fixed to 1:1.

### **3.4. Formation of micro size emulsion**

The life and effectiveness of ELM used for CO<sub>2</sub> separation from the gas stream depends upon its stability and pH. The major factors affecting the stability of the w/o ELM are the types of surfactant, method of preparation, pH, phase volumes, and the concentration of constituents [19]. To produce a stable ELM, the influence of the Span-80 concentration, speed of emulsification, and time on EDS was assessed extensively. The concentration of surfactant, NaOH, and extractant plays an essential role on the EDS, whereas the stability of the ELM is relevant to the EDS. In this study, the pH of the emulsion was reported to be an important factor affecting the stability of the emulsion, which was mostly ignored in previous studies. The effects of NaOH on the pH of the emulsion and the effect of pH over the stability of the emulsion were investigated. Before applying the ELM to the RDC system, the optimal values of the EDS, such as the concentrations of the surfactant, extractant, and NaOH, were assessed.

A high performance disperser, Ultra Turrax<sup>®</sup> T25 (made in IKA, Germany), high-speed homogenizer with an 18G mixing shaft was used to produce the micro size emulsion droplets. Ultra Turrax<sup>®</sup> T25 dispersed the aqueous phase into the organic phase. The homogenizer shaft was made of a hollow cylinder containing a rotor inside connected to the motor and stator with



teeth on the outside. The membrane phase was prepared in a 100 ml beaker by mixing the diluent phase. Initially, the speed was fixed to 10000 rpm and the internal aqueous stripping phase was poured drop wise. After adding the internal phase (w) to the organic phase (o), the speed of the disperser was increased to 20,000 rpm. Time intervals of 1, 2 and 3 hours were used for each sample preparation.

#### 4. Characteristics of the ELM

ELM was prepared with a water oil ratio of 1:1 at different concentrations of surfactant and extractant, different emulsification speeds, and emulsification times to determine their effects on the particle size diameter, stability, pH, and conductivity. **Table 1** lists all the variables.

**Table 1.** Values and Parameters for 1:1 w/o ELM Formulation

NaOH (M)	Extractant (% v/v of water)	Surfactant (% v/v of total)	Emulsification speed (rpm)	Emulsification Time (Min)
0.1	2	2	10000	60
				120
				180
			15000	60
				120
				180
	4	4	20000	60
				120
				180
			10000	60
				120
				180
6	6	15000	60	
			120	
			180	
		20000	60	
			120	
			180	
6	6	10000	60	
			120	
			180	

	120
	180
	60
15000	120
	180
	60
20000	120
	180

#### 4.1. Particle size diameter

An optical electronic microscope (Olympus® BX 50, Olympus Optical Co., Ltd. Tokyo, Japan) was used to analyze the size of the emulsion droplets. Images of the sample were taken using the Five Digital Imaging System and the particle size was analyzed using Soft Imaging System Analysis Auto Five (SISauto) software. The software is capable of developing the image and preparing the statistical data to determine the mean particle size, median, minimum, and maximum droplet size as well as the sum of the particle size.

#### 4.2. Phase Stability

The stability of ELM was determined by its constant behavior of dispersity and the uniform distribution of the dispersed phase with respect to time. The molecular attraction forces are responsible for maintaining the phase stability. The formation of larger aggregates due to coagulation or flocculation caused phase instability resulting in phase separation.

To determine the emulsion phase stability, the scaled test tubes were filled with a sample of the emulsion and the emulsion was allowed to settle at room temperature (25°C). After 24 hours, the phase separation ratio of the water and oil was calculated using the following equation:

$$\text{Stability \%} = \frac{V_t - V_w}{V_t} \times 100 \quad (1)$$

where  $V_t$  is the total volume of the emulsion in the test tube,  $V_w$  is separated volume of the aqueous internal phase in the test tube. The surfactant concentrations, emulsification time, and speed were varied, and the parameters for a stable emulsion were identified for further investigations. These parameters were used to prepare the ELM for further evaluation of CO<sub>2</sub> removal in the RDC system.

### **4.3. pH analysis**

pH analysis is a useful tool for analyzing the concentration difference of the membrane and feed phase [20]. The pH of the w/o emulsion were recorded to determine the optimal ELM system. The difference in pH between the receiving phase and the feed phase is the driving force of the ELM mass transport system. Because of the concentration gradient, the complex was then transferred to the interface of the internal phase. The initial release of electrolytes entrapped in the internal aqueous phase was determined using a pH meter. HANNA instruments Malaysia Sdn. Bhd. A Bench pH 210 was used to measure the H<sup>+</sup> concentration of the ELM for each sample after emulsification.

### **4.4. Emulsion droplet size**

Measuring the size of an emulsion droplet is one of the important characteristics for analyzing the overall surface area of the ELM. The internal surface area of the emulsion with a micron droplets size can be measured using the photographic image [21]. Electronic microscopy image processing and image analysis is one of the most authentic and latest methods of identifying the emulsion droplet size [22]. The mean diameter of the emulsion droplet of each ELM sample prepared for this study was measured using an electronic microscope attached to the SIS auto Image analyzing software. An optical electronic microscope was used to analyze the size of the

emulsion droplet. To prepare the w/o emulsion, the energy and surfactant are the basic requirements to increase the interfacial area of the bulk aqueous phase by dispersing it into an organic phase. The emulsion samples, prepared using the specifications given in **Table 2** were analyzed to examine the influencing parameters on the droplet size. **Fig. 3** presents images of the ELM sample. Using 2, 4 and 6% Span-80, an emulsification speed of 10000 rpm and 60 min were obtained on the optical microscope photograph with a 100X magnification. The mean diameter of the emulsion droplet decreased with increasing Span-80 concentration.

**Table 2.** Specifications of the w/o Emulsion

Phase Composition	Specifications
Membrane phase	30°C at 700 rpm for 15 minutes
Kerosene	100 ml
Span-80	2, 4 and 6 % V/total volume
Internal stripping phase	30°C at 700 rpm for 15 minutes
Water	100 ml
NaOH	0.1M
Emulsification time	60, 120 and 180 minutes
Speed	10000, 15000 and 20000 rpm

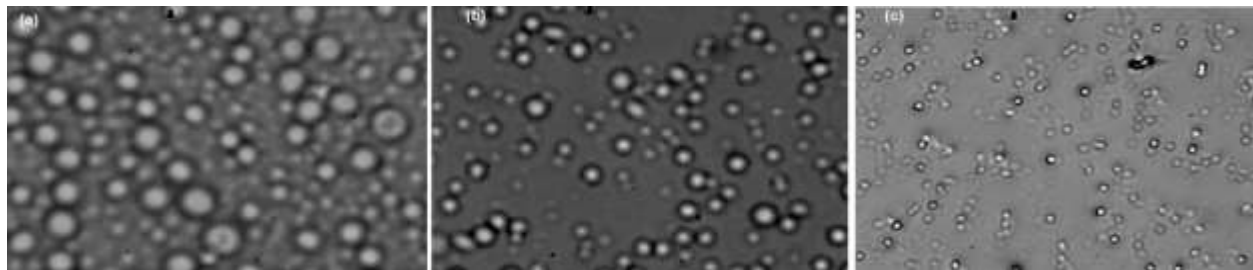


**Fig. 3.** Optical microscopy image at 100X magnification, emulsification speed of 10,000 rpm and 60 min using (a) 2% Span-80 (b) 4% Span-80 (c) 6% Span-80.

## 5. Parametric Study

The concentration of the constituents, emulsification time, and speed are the most important parameters affecting the EDS and the stability of the emulsion. These parameters were studied to develop an effective ELM.

### 5.1. EDS analysis

#### 5.1.1. Effect of emulsification time

The emulsification time is related to the amount of energy consumed by the emulsifying chamber during the emulsification process. Increasing the emulsification time reduces the size of the emulsion droplet [23, 24]. A previous study reported that 99.9 % of the emulsification energy is dispersed as heat and only 0.1 % is applied to the production of emulsion droplets [25]. Therefore, to control the effect of heat generation due to the longer emulsification, a water-cooling bath was used to maintain an emulsion temperature of 25°C.

In this study, to determine a suitable emulsification time for the minimum droplet size, a series of measurements were carried out on several samples for 60, 120 and 180 minutes emulsification. A sample of the ELM prepared at 10,000 rpm containing 2% Span-80 showed that the mean emulsion droplet size decreased with increasing emulsification time. **Fig. 4** shows that for 60-minute emulsification, the mean droplet size was 2.98  $\mu\text{m}$ , whereas it was reduced to 2.91  $\mu\text{m}$  after 180 minutes. Similar behavior was observed using 4 and 6% Span-80. This suggests that a longer emulsification time can reduce the emulsion droplet size. Mabile, Leal-Calderon [26] reported that the shearing time reduces the emulsion droplet diameter abruptly and it continues the deformation of the initial droplet further into small fragments. A similar pattern of

continuous reduction in the emulsion droplet size with time for each sample of the ELM was observed.

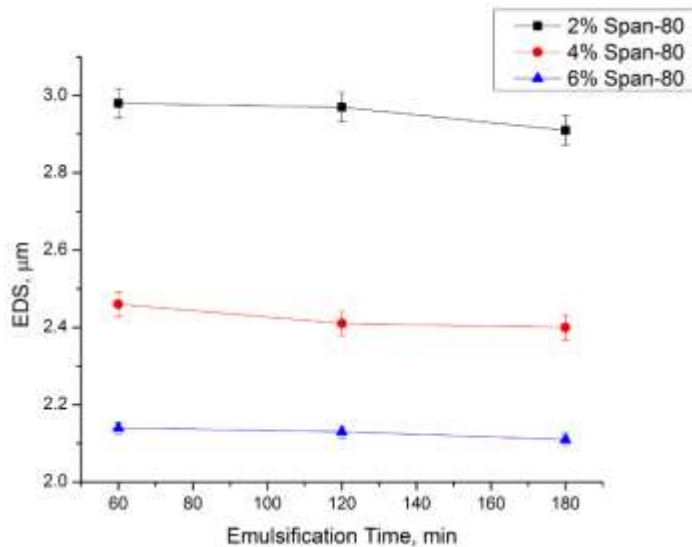


**Fig. 4.** Effect of the emulsification time on EDS at 10,000 rpm

### 5.1.2. Effect of emulsification speed

A decrease in the mean droplet size of the emulsion and the change in the size distribution of the emulsion droplet is achieved by high-speed emulsification [27-31]. The emulsification speed is a force applied by the homogenizer to deform or disperse the liquid. The droplet deformation is caused by the velocity and stress applied to the emulsion [32]. As more stress is applied, small emulsion droplets are produced. The speed is considered to be the hydrodynamic pressure applied by the homogenizer to pass the liquid through the narrow channels of the grind mill or homogenizer shaft [33]. The continuous pressure applied by the homogenizer on the liquid passed through the narrow channels caused a decrease in the mean droplet size. Increasing the emulsification speed caused an increase in the net power density because of the mechanical

energy input. The breakup of an emulsion droplet is possible only at high power density values [34]. The high speed produced a small sized emulsion droplet while dispersing the aqueous phase into the organic phase. The effects of the emulsification speed was studied experimentally. The results presented in **Fig. 5** indicates that the mean emulsion droplet was 2.91  $\mu\text{m}$  using 2% Span-80 at 10000 rpm, whereas it decreased to 2.56  $\mu\text{m}$  at 20,000 rpm. A similar trend was also observed by sample containing 4% Span-80. On the other hand, using 6% Span-80, the EDS decreased rapidly after 15,000 rpm, in which EDS was reduced to 1.44  $\mu\text{m}$  at 20,000 rpm. This finding is in contrast to that reported by Raikar, Bhatia [33]. This indicates that shear force generated due to the emulsification speed is only useful when a proper amount of surfactant is available in the emulsion constituents. The effect of the emulsification speed suggests that a high rotational speed of the homogenizer produces shear stress inside the flowing area of the fluid. Therefore, in the presence of an emulsifier, small droplets will be formed at a high emulsification speed.

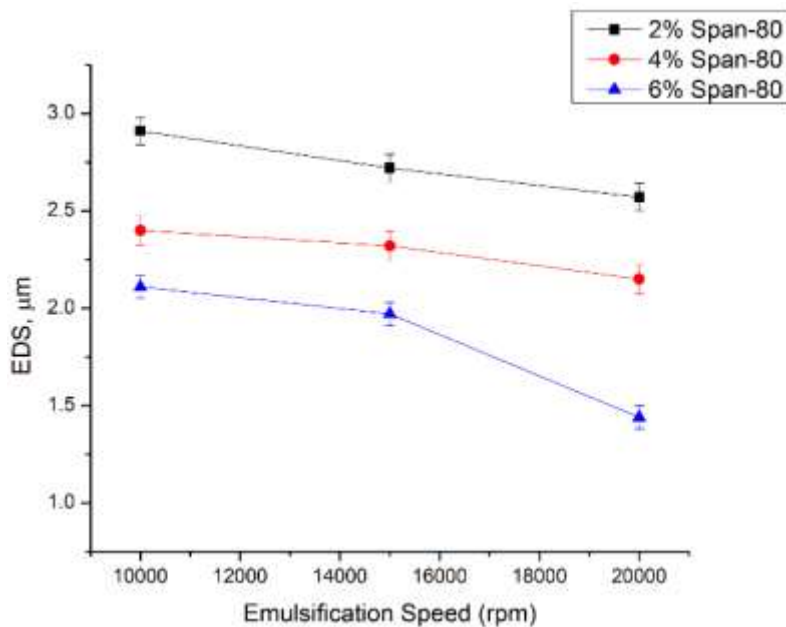


**Fig. 5.** Effects of the Emulsification speed on EDS after 180 min

### 5.1.3. Effect of concentration of Span-80

The interfacial surface tension of the surfactant controls the resistance of the emulsion droplet to deform into fragments due to the extent of its pressure difference [35]. A significant change in the interfacial tension of the emulsion is based on the surfactant ratio [36]. Increasing the surfactant concentration up to 6% decreased the EDS linearly, but above this value, the reverse trend in the droplet size was reported [37]. The effect of Span-80 concentration on the emulsion droplet was previously examined to validate the effects of other parameters, such as the emulsification time and speed, on the surfactant ratio [38]. In this study, the effects of the surfactant concentration over the EDS in relation to time and speed were determined. **Fig. 6** shows the effects of the Span-80 concentration on the EDS as a function of the speed and time.

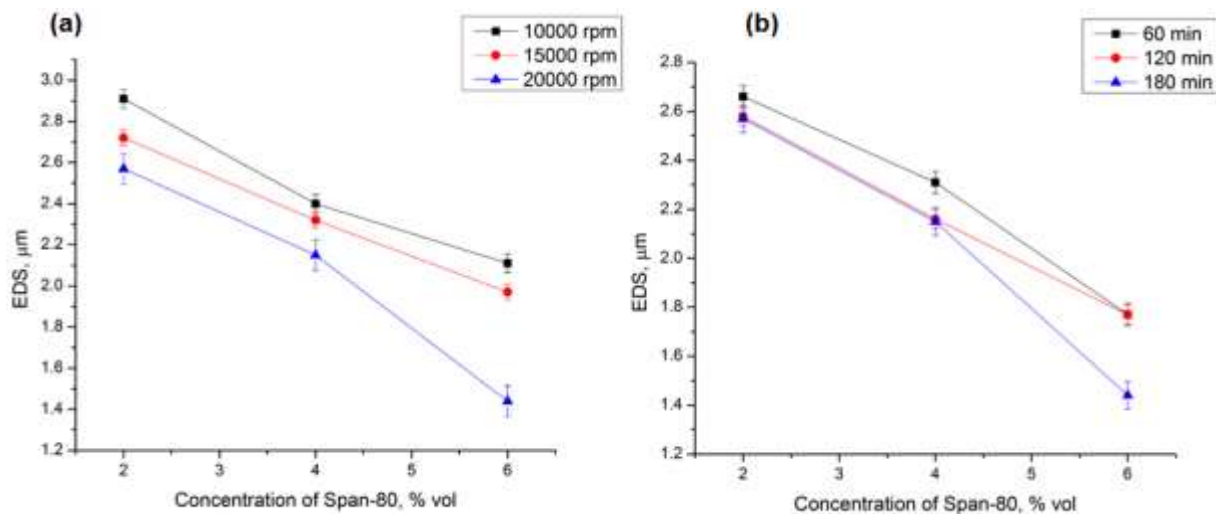


**Fig. 6.** Effect of (a) concentration of Span-80 and emulsification speed on EDS at 180 min (b) concentration of Span-80 and emulsification time on EDS at 20,000 rpm



**Fig. 6 (a)** indicates that at 10,000 rpm, the EDS was reduced sequentially from 2.98 to 2.11  $\mu\text{m}$  by increasing the concentration of Span-80 from 2 to 6%. With increasing Span-80 concentration, a similar trend of a decrease in the mean diameter of the emulsion droplet was observed for 15,000 rpm. In contrast, the mean EDS for 20,000 rpm differed from the others. Increasing the surfactant concentration affected the rheological behavior of the emulsion. Therefore, such a phenomenon is probably due to the change in the rheological behavior of the emulsion as the amount of Span-80 increases. For 6% Span-80, more energy is required for further deformation, and while applying the 20,000 rpm, the energy intensity of the system could deform the droplet into a smaller size. Opawale and Burgess [39] also reported that Span-80 is elastic in nature with organic compounds. Therefore, the elasticity of emulsion increased by increasing the Span-80 concentration. As mentioned by Derkach [40], the emulsion droplet is deformed rapidly when elastic emulsions are exposed to high speed emulsification. A similar phenomenon was observed as the emulsion droplet was decreased to 1.48  $\mu\text{m}$  for a sample containing 6% Span-80 at 20,000 rpm.

**Fig. 6(b)** presents the mean droplet diameter of the emulsion samples using different concentrations of Span-80 at different emulsification times at 20,000 rpm. The ELM sample containing 2% Span-80 deformed to produce a 2.66  $\mu\text{m}$  mean diameter of the EDS after 60 minutes emulsification time. This was reduced to 2.31  $\mu\text{m}$  using 4% Span-80, and the emulsion droplet size further reduced to 1.77  $\mu\text{m}$  when the concentration of Span-80 was increased to 6%. A similar trend was observed using 2, 4 and 6% of Span-80 for 120 minutes emulsification time. After extending the time to 180 minutes, the result shows that for 2% and 4% Span-80, the EDS was 2.57  $\mu\text{m}$  and 2.15  $\mu\text{m}$ , respectively, whereas it was decreased to 1.44  $\mu\text{m}$  for ELM sample

containing 6% Span-80. These results suggest that during the formation of a droplet, the surfactant is adsorbed on the interface of the newly generated droplet, which decreases the interfacial tension of the dispersed phase, resulting in a further decrease in emulsion droplet diameter.

The difference in the decreasing trend of EDS after a 180 min emulsification time using 6% Span-80 showed that at higher surfactant concentrations, the droplet deformation time was increased due to the viscosity of the emulsion. This shows that the surfactant has a major impact on the EDS, but it also depends on the emulsification speed and time. Increasing the surfactant concentration decreases the mean EDS but increases the interfacial area. The interfacial surface tension of the emulsion droplet was decreased by increasing the Span-80 concentration due to the larger decrease in emulsion droplet. These results show that the Span-80 concentration, emulsification time and speed have a significant effect on the EDS, and all the parameters are interrelated. A variation of any of above parameters will affect the EDS.

#### **5.1.4. Effect of extractant**

A series of experiments were conducted to determine the optimal concentration of TEA to formulate a stable ELM with the minimum EDS for CO<sub>2</sub> separation in the RDC system. To determine relationship among the emulsification time, speed and Span-80 concentration, samples of the ELM were prepared by varying the volume % of TEA. The volume of Span-80 was 4% of the total volume of the emulsion, whereas the volume of TEA was 2, 4 or 6% of the volume of the aqueous phase. The effect of the TEA concentration on the EDS was analyzed together with various emulsification speeds and times because the emulsification time and homogenization speed was identified as a relative factor while analyzing the effects of Span-80 on the EDS.

Different samples of the emulsion were prepared with an emulsification speed of 10,000, 15,000, and 20,000 rpm for 60, 120, and 180 minutes using the composition and specifications given in **Table 3**. **Table 4** lists the emulsion droplet size for the different surfactant concentrations at different emulsification speeds and emulsification times, whereas **Table 5** presents the emulsion droplet size at different emulsification speeds and emulsification times in the absence of a surfactant.

**Table 3.** Composition of the water in oil (w/o) emulsion

Phase Composition	Specifications
Membrane phase	30 °C at 700 rpm for 15 minutes
Kerosene	100 ml
Span-80	0
Internal stripping phase	30 °C at 700 rpm for 15 minutes
Water	100 ml
NaOH	0.1M
TEA	2, 4 and 6% Volume

**Table 4.** Emulsion droplet size with the surfactant concentration

Surfactant (% v/v of total)	Emulsification speed (rpm)	Emulsification time (Min)	EDS ( $\mu\text{m}$ )
2	10,000	60	2.98
		120	2.97
		180	2.91
	15,000	60	2.84
		120	2.8
		180	2.72
	20,000	60	2.66
		120	2.58
		180	2.57
4	10,000	60	2.46
		120	2.41
		180	2.4

		60	2.36
	15,000	120	2.32
		180	2.32
	20,000	60	2.31
		120	2.16
		180	2.15
	10,000	60	2.14
		120	2.13
		180	2.11
6	15,000	60	2.07
		120	1.98
		180	1.97
	20,000	60	1.77
		120	1.77
		180	1.44

**Table 5.** Emulsion droplet size without a surfactant

<b>Extractant (% v/v of water)</b>	<b>Emulsification speed (rpm)</b>	<b>Emulsification time (Min)</b>	<b>EDS (<math>\mu\text{m}</math>)</b>
		60	3.33
	10,000	120	3.32
		180	3.24
	15,000	60	2.97
2		120	2.92
		180	2.66
	20,000	60	2.57
		120	2.55
		180	2.52
	10,000	60	2.42
		120	2.41
		180	2.38
4		60	2.29
	15,000	120	2.21
		180	2.2
	20,000	60	2.2

		120	2.14
		180	2.13
		60	2.12
	10,000	120	2.07
		180	1.98
		60	1.97
6	15,000	120	1.72
		180	1.66
		60	1.61
	20,000	120	1.57
		180	1.5

#### 5.1.5. Effect of the TEA concentration on the EDS

To examine the effects of the TEA concentration on the EDS, various emulsion samples were prepared without adding a surfactant, while using 2, 4 and 6% volume of TEA. In previous studies, the surfactant was considered to be the influencing parameter determining the emulsion droplet size [32, 33, 41], whereas the effect of the extractant on the emulsion droplet has not been reported. On the other hand, it was reported that TEA can exhibit high interfacial activity owing to its lipophilic nature [42, 43]. Therefore, in this study, the comparative analysis of TEA, with and without Span-80, was conducted to examine its effects on the EDS. Using a 2, 4, and 6% volume of TEA, the emulsion samples were prepared by changing the emulsification time and speed.

**Fig. 7** shows the effects of the TEA concentration on the emulsion droplet at 10,000, 15,000, and 20,000 rpm, respectively. The concentration of TEA has a linear effect on the EDS. The ELM prepared with a 2 % volume of TEA at a speed of 10,000 rpm for 60 minutes of homogenization of the EDS was 3.33 $\mu$ m. Increasing the TEA to 6% volume at the same speed and emulsification

time resulted in a decrease in the emulsion droplet size to 2.12  $\mu\text{m}$ . The same trend of the reduction in mean EDS was observed for emulsification times of 120 and 180 minutes. An increase in the TEA concentration alters the viscosity of the emulsion, which modifies the effects of the emulsification time and speed on the EDS. Increasing the TEA concentration causes an increase in the absolute viscosity of ELM, which requires more energy for further deformation of the emulsion to reduce the droplet size [44]. Pandolfe [45] reported that the emulsification efficiency of emulsifying equipment decreases with increasing viscosity of the emulsion. For higher TEA concentrations, large amounts of energy and force are required to reduce the emulsion droplet size. The results obtained after this analysis suggest that TEA has a prominent effect on the EDS in relation to the emulsification time and speed.

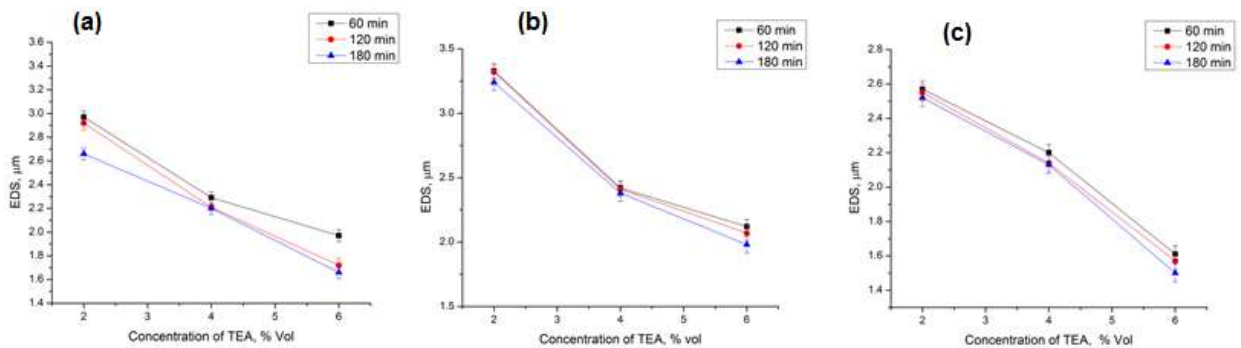


**Fig. 7. (a)** Effects of the TEA Concentration on EDS at 10,000 rpm (b) 15,000 rpm and (c) 20,000 rpm.

The interfacial tension of the surfactant impedes the deformation of the emulsion droplet, which affects the droplet size [35]. Comparative analysis of the EDS with and without a surfactant was conducted to assess the effect of TEA on EDS. Emulsion samples were prepared using 2, 4, and 6% TEA with an equal percentage of Span-80 and without Span-80. The emulsification speed and time were fixed to 20,000 rpm and 180 minutes, respectively.

**Fig. 8** shows that the emulsion droplet is larger without a surfactant and it decreased when an equal volume percent of Span-80 was added. Using 2% Span-80, the EDS was 2.91  $\mu\text{m}$  while after addition of 2% TEA the EDS increased to 3.24  $\mu\text{m}$ . Similarly, each sample of the emulsion without TEA has a small EDS, which increased with the addition of TEA. TEA affects the interfacial surface tension of the emulsion; therefore, the emulsion droplets cannot deform more into a small size. The emulsion droplet size was decreased by increasing the TEA concentration, but compared to the sample containing Span-80, the mean diameter of the emulsion droplet was higher for each sample containing TEA.

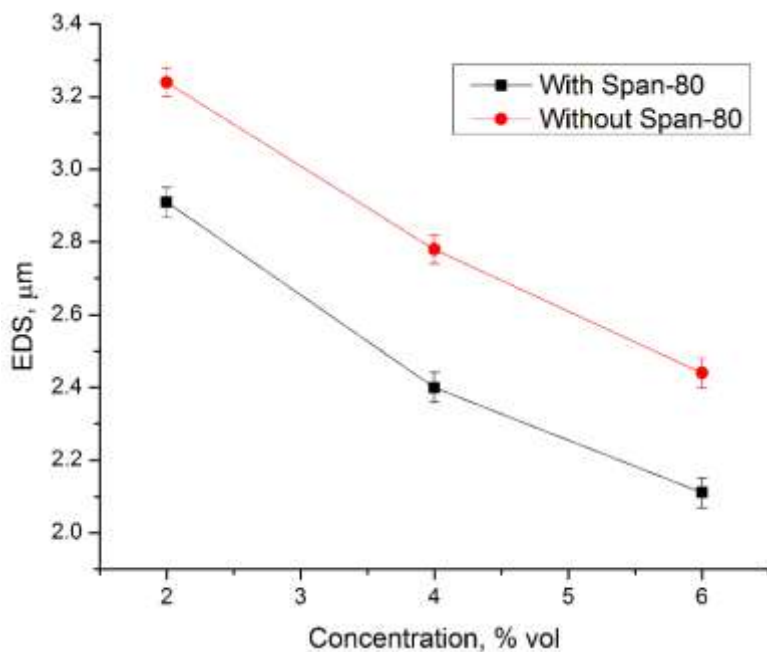


**Fig. 8.** Comparative effect of concentration on the EDS with and without Span-80

The results indicate that to maintain the EDS, the concentration of extractant must be determined by the correlation of the surfactant. Therefore, that the concentration of Span-80 and the emulsification speed have major effects on the EDS; the size of the emulsion droplet was

reduced significantly by increasing the volume percentage of Span-80 and speed of homogenization. Liu et al [46] observed a similar effect of Span-80 over the EDS. A steady decrease in the average size of the emulsion droplet was observed by increasing the Span-80 to 6% due to the effect of Span-80 on interfacial surface tension of the emulsion droplet. The emulsification time, as an independent variable, did not an effective role in the reduction of EDS, but it is a relative factor depending on the overall viscosity of the emulsion. The extractant has a significant effect on the EDS. The size of emulsion droplet size increased with increasing amount of TEA due to the increase in ionic charge on the emulsion droplet surface. Increasing the amount of surfactant also helps in reducing the emulsion droplet size.

#### 5.1.6. Effect of NaOH and TEA on pH

The emulsion sample was prepared using the parameters shown in **Table 6** to examine the effect of the concentration of TEA and NaOH on the pH of the ELM. The results are shown in **Fig. 9**.

**Table 6.** Composition of the w/o Emulsion

Phase Composition	Specifications
Membrane phase	30°C at 700 rpm for 15 minutes
Kerosene	100 ml
Span-80	2,4 and 6% V/total volume
Internal stripping phase	30°C at 700 rpm for 15 minutes
Water	100 ml
NaOH	0.1, 0.2, 0.3, 0.4 and 0.5 M
TEA	2,4 and 6% V/Water Volume

**Fig. 9(a)** shows the ELM sample prepared with 0.1 M of NaOH; the pH value at 2% TEA was 10.99 whereas the pH value increased to 11.10 by increasing the TEA concentration to 6%. A similar effect of an increase in pH of the ELM was observed for the each sample with various molar concentrations of NaOH. The linear trend of **Fig. 9 (b)** shows that the molar concentration



of NaOH has a strong effect on the pH for all the ELM samples containing 2, 4 and 6% TEA. Using 0.1 M NaOH, the pH of the ELM was 10.99 for 2% TEA, which was increased to 12.60 by increasing the NaOH concentration to 0.5 M.

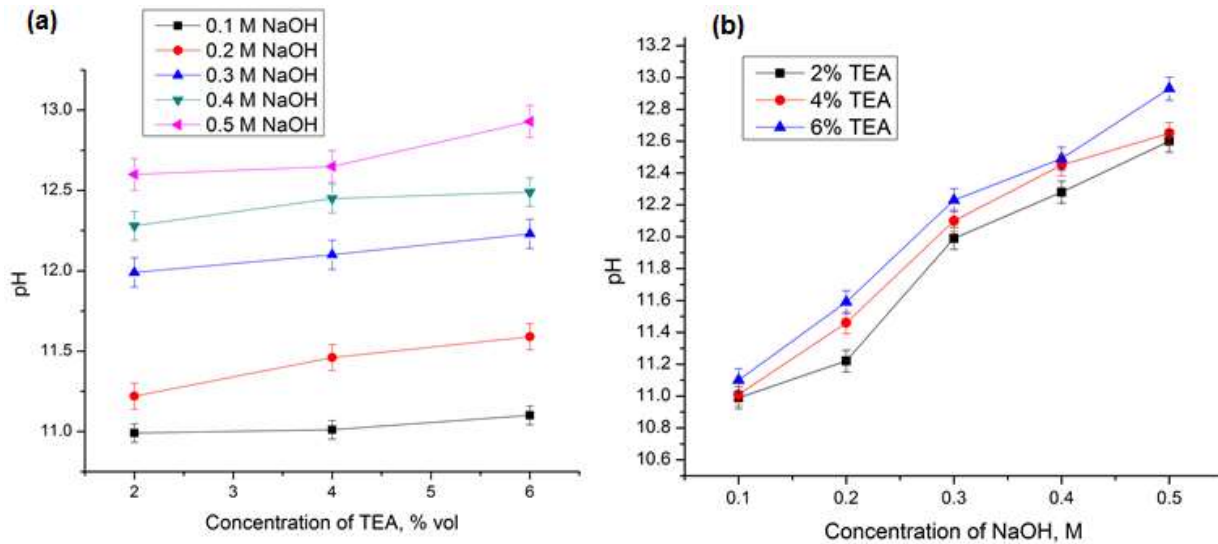


**Fig. 9.** Effect of the Concentration (a) TEA and (b) NaOH on pH

This indicates that compared to TEA, free hydroxide ions in NaOH, are more active in increasing the pH of the ELM. This supports the use of NaOH as a stripping agent for CO<sub>2</sub> absorption in a RDC system. The pH of the ELM composition was increased by increasing the NaOH concentration in the pre-emulsion aqueous phase of the emulsion [47]. TEA is a strong base; the pH of ELM is increased by increasing its concentration in the aqueous phase. NaOH and TEA containing hydroxide ions as a strong base [48], the release of hydroxide ions in the emulsion increases the pH. This increase in the pH of the ELM helps to manage the substance according to the need of the system application

## 5.2. Emulsion stability analysis

An emulsion is an unstable mixture of two liquids that do not normally mix, such as oil and water. An emulsifying agent is needed to form a stable mixture of two repelling liquids, which will prevent the oil droplets from coalescing and separating from the opposing liquid. The shelf life of the emulsion after preparation is known as the stability of the emulsion, which is one of the important parameters. This study examined the effects of pH, EDS and concentration of the surfactant on the stability of ELM. Considering all parameters discussed in the previous sections, the emulsion was prepared using the composition and specifications listed in **Table 7**. The samples were prepared at 20,000 rpm for a 120 minute emulsification time. The samples were analyzed for their stability by changing the concentration of Span-80.

**Table 7.** Composition of the w/o Emulsion

Phase Composition	Specifications
Membrane phase	30°C, 700 rpm, 15 minutes
Kerosene	100 ml
Span-80	2,4 and 6% V/total volume
Internal stripping phase	30°C, 700 rpm, 15 minutes
Water	100 ml
NaOH	0.1M
TEA	6% V/Water Volume

### 5.2.1. Effect of pH

The pH of various samples was used to plot a graph against the stability of the emulsion. The stability was determined by measuring the volume fraction of the water phase, separated from the organic phase of an emulsion. **Fig. 10** shows that the emulsion is totally stable at pH 10 - 11.5. At this value, no separation of the water phase from the oil phase was observed after 24 hours at room temperature. The emulsion stability decreased suddenly when the pH of the

aqueous phase was adjusted to 12 and above. Yang and Niu [49] reported that excess negative charges on the interface of the w/o emulsion, caused by  $\text{OH}^-$  ions from the aqueous phase decreases the stability of emulsion [50]. The decrease in the stability of the emulsion at high pH is probably due to a decrease in the negative charges on the interface of the water droplets dispersed in the w/o emulsion caused by the addition of NaOH and TEA. The zeta potential of the dispersions has a strong effect on the stability of the emulsion liquids [49]. Increasing the pH of the emulsion, the zeta potential of droplet is decreases.

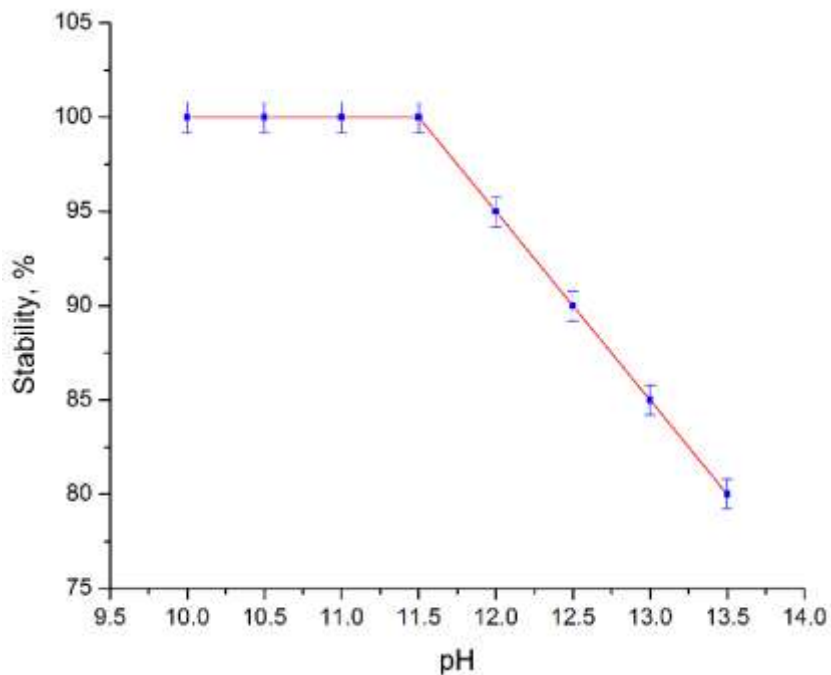


**Fig. 10.** Effect of pH on the stability

According to Ren and Zhang [51], the pH of the internal stripping phase and continuous feed phase affects the separation efficiency and mass transfer flux. A higher concentration difference may improve the separation of acidic gases because the pH will influence the mass transport of the solutes. A higher pH leads to a higher concentration difference, which increases the

separation of acidic gases in any gas mixture. The pH of the emulsion was increased by increasing the NaOH concentration, but the stability decreased significantly. A suitable composition of ELM containing NaOH and TEA with the maximum stability is important for CO<sub>2</sub> separation.

### 5.2.2. Effect of droplet size

**Fig. 11** shows the effects of the emulsion droplet size on the stability of the emulsion. The emulsification speed and time were constant for all samples, i.e. 20,000 rpm and 120 minutes, respectively.

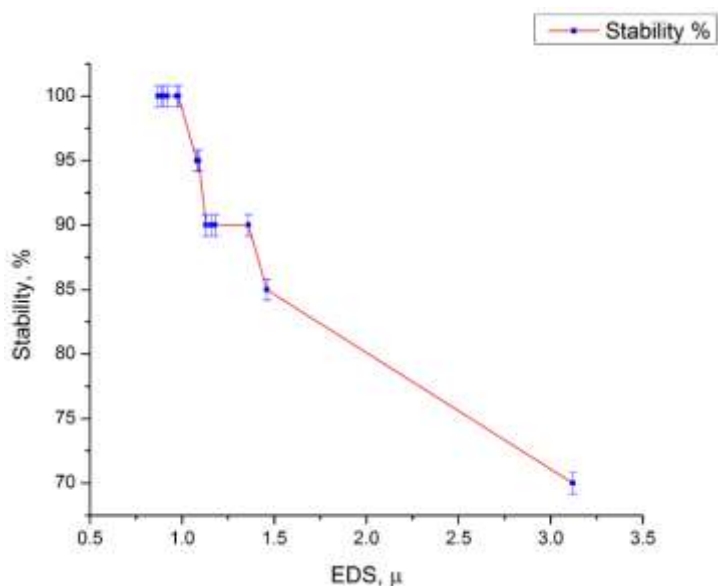


**Fig. 11.** Effects of the EDS on Stability.

The results for the mean diameter show that below 1  $\mu$ m, the emulsion is highly stable but above this value, the stability of the emulsion was reduced. As reported by Katsuroku and Fujio [52] and Walstra [23], deformation of the emulsion droplet into a smaller size is a function of the emulsification time and speed and the concentration of surfactant. The emulsion droplet mean

diameter was reduced by increasing the Span-80 concentration. Therefore, the stability of emulsion was enhanced due to the increase in interface surface tension of the emulsion droplet.

The effects of EDS on the stability proves that the maximum number of emulsion droplets, with small mean size and wide size distribution, show very less coalescence. **Fig. 11** shows that the emulsion stability increased with decreasing mean droplet size and below 0.89  $\mu\text{m}$ , it was constantly stable for 24 hours at room temperature. In a highly homogenized w/o dispersion system, a small droplet size results a large specific interfacial area, which maintains the stability of the emulsion [53]. This is because the stability of the emulsion is increased with a small droplet size, as small droplets require more time to coalesce and separate into the phases of the emulsion [54]. With a small droplet size, the emulsions are more stable than the large droplets [55]. A small droplet size and high zeta potential resists aggregation; therefore, the stability of the emulsion is increased [50, 56]. The quantity of droplets is increased when small size fractions of EDS are produced, which increases the coalescence time.

### **5.2.3. Effect of Span-80**

The surfactant is a non-ionic substance that decreases the interfacial tension between the phases of the emulsion. On the other hand, the extractant and internal stripping aqueous phase increase the ionic charge of the emulsion. The concentration of surfactant and stripping agent, i.e., Span-80 and NaOH, also has a significant effect on the stability of ELM. **Fig. 12** shows that the stability of the emulsion increases with increasing concentration of Span-80 and the stability of the emulsion decreases with increasing NaOH concentration in the aqueous phase.

Using 2% Span-80, the emulsion was 100% stable with 0.1, 0.2 and 0.3 M of NaOH, but the stability was decreased considerably with further increases in the NaOH concentration. A similar effect was observed for 4 and 6 % Span-80 using 0.1 and 0.2 M of NaOH because the stability of the emulsion increases as it prevents the droplets from coalescing. Increasing the concentration of NaOH in the pre-emulsion aqueous phase increases the interfacial surface tension between the organic phase and the dispersed aqueous phase; thus, the stability of emulsion was decreased due to an increase in the interfacial surface tension between the two immiscible phases of the emulsion.

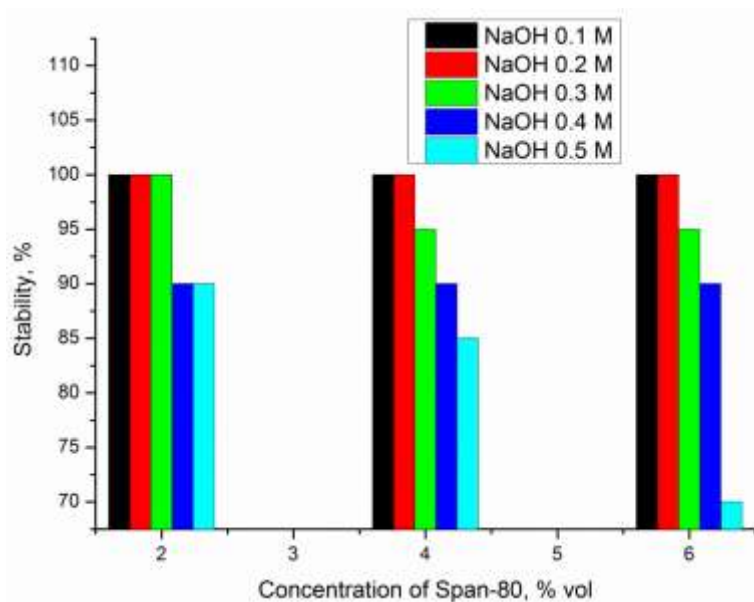


**Fig. 12.** Effect of the concentration of Span-80 on the stability

The results of this study on the effect of the surfactant on the stability of ELM are similar to those reported by Matsumoto [57] and Kamarudin et al. [58] Molecules of the surfactant are adsorbed at the interface of the w/o emulsion to form a protective film around the water droplets dispersed in the organic phase. The interfacial film strength of the emulsion droplet increased

with increasing Span-80 concentration, which prevented the coalescence; thus, the stability was increased [59]. With increasing Span-80 concentration, the droplet size distribution reduced and the mean droplet size of the emulsion decreased below 1  $\mu\text{m}$ , resulting in an increase in the stability of the emulsion. Up to 0.3 M of NaOH, the emulsion was stable for 24 h for each sample containing 2-6% of Span-80, whereas the stability of the emulsion was decreased to 70 % by increasing the NaOH concentration from 0.4 to 0.5.

A similar phenomenon was also reported previously by Barad, Chakraborty [55]. A higher zeta potential is required for a smaller sized emulsion droplet to resist aggregation. Increasing the concentration of NaOH reduces the zeta potential of the emulsion droplets. Therefore, the attraction among emulsion droplets exceeds the coalescence of the dispersed aqueous phase to separate it from the organic phase of the emulsion.

## **6. Performance of a stable ELM to separate CO<sub>2</sub> from natural gas in RDC**

The RDC columns used for the gas-liquid system consist of a series of stages separated by equally spaced horizontal stators and shaft mounted rotor discs. The liquid injected into the reactor from the top and gas phase is injected through a small gas inlet in the bottom near the rim of the rotor. The discs mounted on the shaft provide a larger surface area to the dispersed phase to increase the interfacial contact area for the maximum mass transfer [18].

### **6.1. Selection of RDC for gas-liquid system**

Based on the gas liquid parameters, the gas-liquid flow behavior, retention time, and mass transfer, some modifications were performed in rotating discs, mounted on the shaft and the static rings to redesign the RDC for gas-liquid absorption system. The rotating discs were

mounted with a RW 20 overhead stirrer manufactured by IKA Germany. The performance of various samples of ELM for CO<sub>2</sub> separation were tested in the RDC column using a batch process. In this process, the RDC was filled with the emulsion using a peristaltic pump. The disc rotator was used to stabilize the emulsion in the contactor column. The gas outlet was connected to Agilent 3000A micro-Gas Chromatograph (GC) unit. The micro-GC was connected to the computer to analyze the data. Refinery gas application (RGA) software was used to measure the CO<sub>2</sub> concentration. The experiments were conducted repeatedly using the different ELM samples. Different mixtures of CO<sub>2</sub> and methane were used to examine the separation behavior of CO<sub>2</sub> in the CO<sub>2</sub>/CH<sub>4</sub> mixture. Finally, the optimal formulation of ELM and the effective operational method for the RDC rig was identified. **Fig. 13** presents a schematic flow diagram of the process.



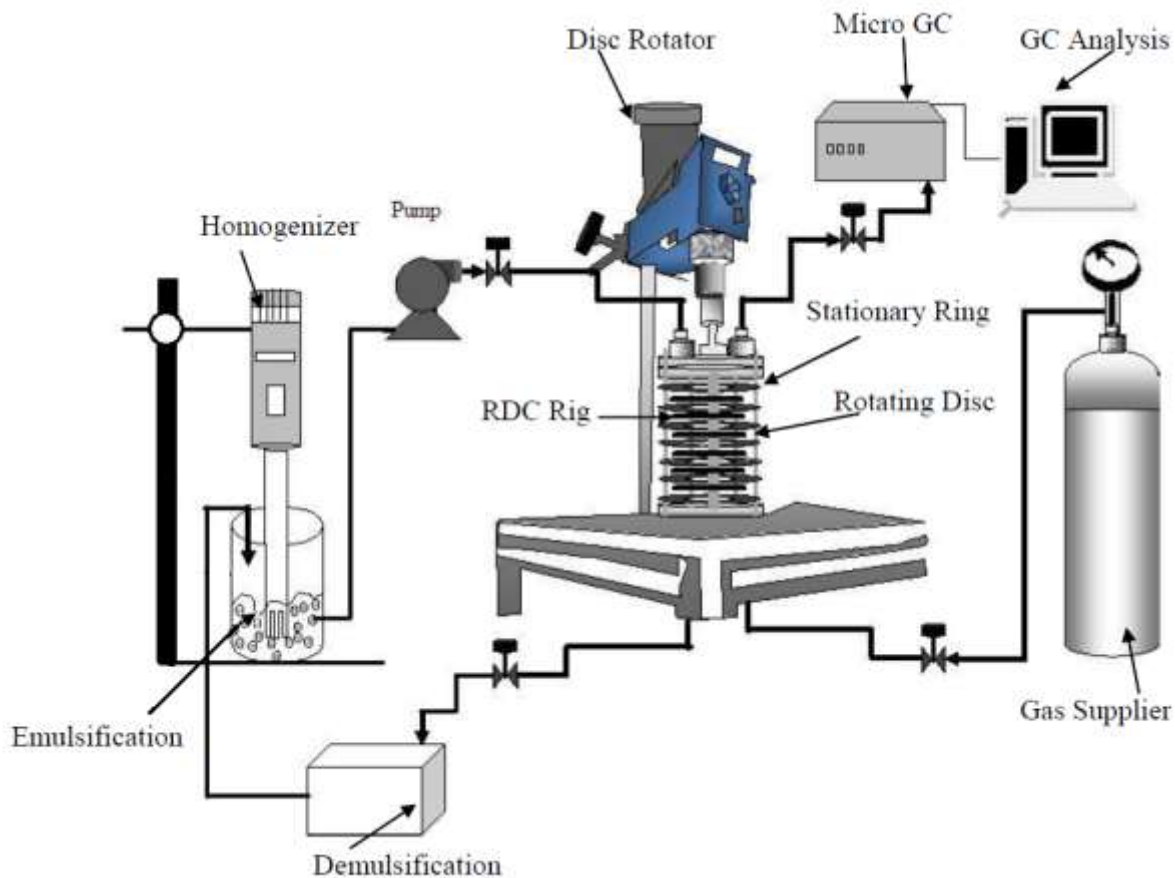


**Fig. 13.** Schematic flow diagram of the RDC rig

The Agilent 3000A micro-GC system provides rapid gas analysis at the sampling point. The 3000 micro-GC was equipped with a thermal conductivity detector (TCD), which allows the system to detect very low concentrations (down to 0.8 ppm), making trace-level analysis at the sample site very convenient.

## **6.2. Effect of the TEA concentration on absorption of CO<sub>2</sub>**

The selected samples of ELM were used in the RDC system to determine the effects of an amine based w/o emulsion on the absorption of CO<sub>2</sub>. A pre-emulsion aqueous phase was prepared using

0.1, 0.2, 0.3, 0.4, and 0.5 M of NaOH. To analyze the effects of the amine concentration on absorption of CO<sub>2</sub>, ELM samples using 2, 4 and 6% v/v of TEA were prepared separately. The samples were applied to the RDC system for CO<sub>2</sub> absorption. RDC was operated at 300 rpm for 30 minutes. The absorption results for each sample were analyzed by gas chromatography. The results are shown in **Table 8**. Increasing the amine concentration in the dispersed phase of ELM resulted in an increase in the amount of CO<sub>2</sub> absorption with respect to its volume. A similar trend of CO<sub>2</sub> absorption was perceived using DEA or TEA in the dispersed aqueous phase of EM. **Table 8** shows that the ELM containing 2% v/v of TEA absorbs 0.89 moles CO<sub>2</sub> and reaches to 0.96 moles when ELM sample containing 6% v/v of TEA was used.

**Table 8.** Absorption of CO<sub>2</sub> from pure CO<sub>2</sub> using TEA

NaOH	TEA	CO <sub>2</sub> Absorption	
		%mole	mole
M	% v/v		
	2	89.00	0.8900
0.1	4	94.25	0.9425
	6	96.54	0.9654
0.2	2	97.03	0.9703
	4	97.20	0.9720
	6	97.54	0.9754
0.3	2	97.64	0.9764
	4	97.65	0.9765
	6	97.97	0.9797
0.4	2	98.49	0.9849
	4	98.53	0.9853
	6	99.42	0.9942
0.5	2	99.49	0.9949
	4	99.68	0.9968
	6	99.99	0.9999

### 6.3. Effect of NaOH on CO<sub>2</sub> absorption

To observe the effect of the NaOH concentration on CO<sub>2</sub> absorption, samples of ELM using 2% TEA were prepared separately while the aqueous phase was prepared using 0.1, 0.2, 0.3, 0.4, and 0.5 M of NaOH. A different sample was used in the RDC system to assess the CO<sub>2</sub> absorption behavior. For TEA, the absorption of CO<sub>2</sub> increases with increasing NaOH concentration. **Fig. 14** presents the moles of CO<sub>2</sub> absorbed by the w/o emulsion for TEA, which it indicates that NaOH concentration enhanced the CO<sub>2</sub> absorption as the molar concentration of NaOH in the dispersed aqueous phase increases.

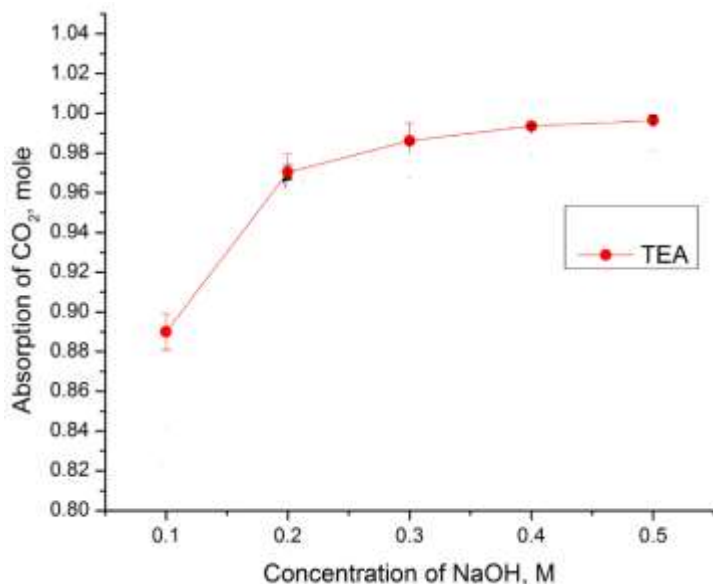


**Figure 14.** Effect of the NaOH concentration on CO<sub>2</sub> absorption using 2% v/v TEA

ELM containing 2% v/v of DEA with 0.1 M of NaOH has very little effect on CO<sub>2</sub> absorption; whereas increasing the NaOH concentration to 0.5 M results in an increase in the amount of CO<sub>2</sub> absorption in the ELM up to 0.99 moles. Similar behavior was observed using 2% TEA as the

extractant in the ELM. By increasing the molar concentration of NaOH, the mass transfer coefficient was increased; therefore, the CO<sub>2</sub> absorption by the dispersed aqueous phase of ELM in the RDC system was increased.

The absorption of CO<sub>2</sub> into an aqueous solution of NaOH, along with an absorbent, such as TEA has been reported [60-62]. In these studies, the rate of CO<sub>2</sub> absorption was increased by increasing the concentration of reactants. Park and Choi [62] reported that the chemical absorption rate of CO<sub>2</sub> in w/o emulsion was increased by increasing the NaOH concentration. A similar effect of the NaOH concentration on the CO<sub>2</sub> absorption in the RDC system was observed. In the ELM system, NaOH forms a layer between the continuous organic phase and the dispersed aqueous phase. At the gas liquid interface, CO<sub>2</sub> makes contact with NaOH and penetrates the droplet and diffuses in the extractant. Considering the initiating role of NaOH over the absorption of CO<sub>2</sub> by the ELM in RDC, the effect of the molar concentration of NaOH on the absorption of CO<sub>2</sub> was examined in this study.

Lin and Chen [63] reported that the molar concentration of NaOH has a linear effect on the CO<sub>2</sub> absorption rate. A similar result was reported by Tedajo and Seiller [64]. Similarly, in the present study, it was found that the absorption of CO<sub>2</sub> increased as the molar concentration of NaOH in the dispersed phase of the ELM was increased from 0.1 to 0.2 M. This significant increase suggests that the aqueous phase concentration of the emulsion developed a pH gradient between the dispersed phase and gas feed phase, which increases CO<sub>2</sub> absorption.

As discussed earlier, a higher molar concentration of NaOH in the aqueous phase increases the pH of the emulsion but decreases its stability. Considering the effect of pH over the absorption

rate of CO<sub>2</sub> in the RDC system, it is favorable to use a higher molar concentration of NaOH in the ELM. At high pH value, however, the stability of the emulsion decreases. Therefore, this suggests that a 0.2 molar concentration of NaOH in the aqueous phase is suitable. Figure 14 shows that there are two regimes of NaOH concentrations in the absorption of CO<sub>2</sub> in the ELM process, rapid and slow. From 0.1 to 0.2 M is the rapid regime and 0.3 to 0.5 M is the slow regime. In the slow regime, a low amount of CO<sub>2</sub> absorption was observed by increasing the NaOH concentration.

#### **6.4. Separation of CO<sub>2</sub> from CH<sub>4</sub>**

Based on the findings of CO<sub>2</sub> absorption in RDC using the ELM prepared with different concentrations of TEA, further studies were conducted to examine the absorption of CO<sub>2</sub> from a (CO<sub>2</sub>/CH<sub>4</sub>) gas mixture. In this work, the separation of CO<sub>2</sub> from the gas pair of CO<sub>2</sub>/CH<sub>4</sub> by ELM using the RDC system was analyzed. Samples of the ELM were prepared by considering the characteristics of the emulsion discussed section 3.1 and the absorption behavior discussed in the previous section. Various samples of the emulsion were prepared using the specifications listed in **Table 9**. These samples were used to examine the CO<sub>2</sub> absorption behavior from a gas mixture. The emulsification speed and time were fixed to 20,000 rpm and 120 minutes, respectively.

Because the absorption of CO<sub>2</sub> in the ELM using RDC system depends on the concentration of extractant in the dispersed aqueous phase and the contact time between the feed gas and emulsion liquid, the effect of TEA concentration, time and RDC speed on the absorption of CO<sub>2</sub> was analyzed to determine the suitable values.

**Table 9.** Specification of the w/o Emulsion

Phase Composition	Specifications
Membrane phase	30°C at 700 rpm for 15 minutes
Kerosene	100 ml
Span-80	4% v/total volume

A mixture of CO<sub>2</sub> and CH<sub>4</sub> gas was prepared by controlling the flow rate and pressure of the gases purged in the RDC. After introducing the ELM in RDC, CO<sub>2</sub> was purged at 8 liters/hr at 25 psi and 25 °C and CH<sub>4</sub> was purged at 6.5 liters/hr at 25 psi and 25 °C to obtain a CO<sub>2</sub> and CH<sub>4</sub> ratio of 0.55/0.45. Using these parameters, the moles of CO<sub>2</sub> and CH<sub>4</sub> were determined by applying the ideal gas law.

According to these calculations, the CO<sub>2</sub> and CH<sub>4</sub> in the RDC were 55 and 45 mole % respectively. Considering the large amount of CO<sub>2</sub> in Malaysian gas reservoirs, a 55/45 ratio of CO<sub>2</sub> in CH<sub>4</sub> was used. On the other hand, the effects of the TEA concentration on CO<sub>2</sub> absorption shows that increasing the amount of extractant in the ELM may influence the absorption efficiency, if the concentration of CO<sub>2</sub> in the mixture is increased. Based on a total 1 mole of gas, the effects of time, concentration, and speed of RDC on CO<sub>2</sub> absorption were analyzed. CH<sub>4</sub> was assumed to be inert in the ELM system and physical absorption of CO<sub>2</sub> from the gas mixture was evaluated experimentally by gas chromatography. An Agilent GC A30000 was used to analyze the CO<sub>2</sub> absorption in the RDC system. Cerity QA-QC software was the basic tool to obtain a computer generated report for the amount of CO<sub>2</sub> and CH<sub>4</sub> present in the exit gas stream from the RDC system.

## 6.5. Effect of time on CO<sub>2</sub> absorption

In this study, the residence time was considered to be the time of the RDC system operated to provide contact between the emulsion and feed gas. The diffusion of CO<sub>2</sub> in this gas-liquid contact system is dependent on the contact time between the feed gas and the dispersed emulsion droplets of the ELM in the RDC. To study this phenomenon, the experiments were conducted to determine the optimized agitation time for the maximum CO<sub>2</sub> absorption in the batch process of the RDC system. The retention time of ELM in the RDC system was between 0 to 30 minutes. The initial time at which the first GC result was obtained is considered time 0. The sample of the outgoing gas stream from the RDC system was purged to GC at 5 minutes intervals. The amount of CO<sub>2</sub> absorbed by the ELM in RDC was calculated based on the CO<sub>2</sub> present in the outgoing stream subtracted from the total amount of feed to the RDC. The speed of the RDC was fixed at 300 rpm for each sample. The results of GC were converted to the amount of CO<sub>2</sub> absorption per volume of the ELM in RDC, and are plotted in **Figure 15**.

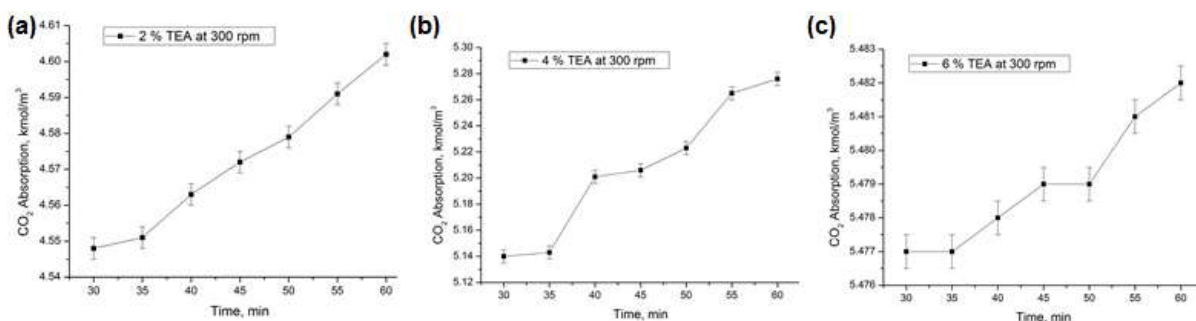


**Figure 15.** Effect of time on CO<sub>2</sub> absorption using (a) 2% TEA (b) 4% TEA and (c) 6% TEA at 300 rpm.

The effect of time on the absorption of CO<sub>2</sub> from the gas mixture of CO<sub>2</sub> and CH<sub>4</sub> was assessed for 2, 4, and 6% v/v of TEA. The amount CO<sub>2</sub> absorbed per volume of the ELM in the RDC column was calculated and is presented in **Table 10**.

**Table 10.** Amount of CO<sub>2</sub> absorbed per volume of the ELM in the RDC column

TEA % v/v	Time	CO <sub>2</sub> absorption kmol/m <sup>3</sup>						
		30	35	40	45	50	55	60
2		4.548	4.551	4.563	4.572	4.579	4.591	4.602
4		5.140	5.143	5.201	5.206	5.223	5.265	5.276
6		5.477	5.477	5.478	5.479	5.479	5.481	5.482

The results of CO<sub>2</sub> absorption were plotted as a function of time to analyze the effect of time on CO<sub>2</sub> absorption. **Fig. 15(a)** indicates that the emulsion containing 2% v/v of TEA absorbed 4.548 kmol/m<sup>3</sup> at the initial time and reached 4.602 kmol/m<sup>3</sup> of CO<sub>2</sub> after 30 minutes operation. **Fig. 15(b)** indicates that CO<sub>2</sub> absorption for the ELM sample containing 4 % v/v of TEA absorbed 5.140 kmol/m<sup>3</sup> at the initial time and reached 5.276 kmol/m<sup>3</sup> after 30 minutes operation. **Figure 15(c)** shows that CO<sub>2</sub> absorption for the ELM sample containing 6 % v/v of TEA absorbed 5.477 kmol/m<sup>3</sup> at the initial time and reached 5.482 kmol/m<sup>3</sup> after 30 minutes operation.

The amount of CO<sub>2</sub> in the outgoing stream decreased with increasing retention time of ELM in RDC. Previous studies by Hagewiesche and Ashour [65] and Brogren and Karlsson [66] on CO<sub>2</sub> absorption in aqueous solutions using scrubbers or gas-liquid absorbers showed that the absorption of CO<sub>2</sub> increased with time. A similar effect of the proportional relation of time with CO<sub>2</sub> absorption in the RDC system was observed. The amount of CO<sub>2</sub> absorption from the gas feed phase in the dispersed aqueous phase increased with increasing contact time in RDC



system. In addition, a high concentration of absorbent in the ELM reduces the time of absorption of CO<sub>2</sub> in the RDC system due to the high concentration difference. In the CO<sub>2</sub>/CH<sub>4</sub> gas mixture, the maximum amount of CO<sub>2</sub> was diffused in the RDC system. Therefore, at a lower TEA concentration, the maximum separation of CO<sub>2</sub> from CH<sub>4</sub> can be achieved by extending the contact time between the feed gas and the aqueous dispersed phase of ELM in RDC.

### **6.6. Effect of TEA Concentration on CO<sub>2</sub> absorption**

The amount of CO<sub>2</sub> absorption in the ELM at 300, 500, and 700 rpm was calculated after 30 minutes operation time of RDC system for 2, 4, and 6% TEA. The CO<sub>2</sub> absorption per volume of ELM was plotted as a function of the TEA concentration and presented in **Fig. 16** for 300, 500 and 700 rpm of RDC. Based on the results obtained for the different speeds of RDC, the amount of CO<sub>2</sub> absorption increased with increasing TEA concentration in the dispersed aqueous phase of ELM. **Fig 16** shows that at 300 rpm of RDC, 4.6 kmol/m<sup>3</sup> of CO<sub>2</sub> was absorbed by the ELM using 2% v/v of TEA, whereas the absorption of CO<sub>2</sub> increased to 5.5 kmol/m<sup>3</sup> using 6% TEA concentration in the ELM.

This shows that by increasing the volume of TEA to 6% in 200 ml of the ELM, the CO<sub>2</sub> absorption capacity was increased to 0.9 kmol/m<sup>3</sup>. A similar effect of the TEA concentration on the absorption of CO<sub>2</sub> in the RDC system was observed at higher values of 500 and 700 rpm. On the other hand, a significant increase in CO<sub>2</sub> absorption was observed with increasing TEA concentration from 2% to 4%, but the absorption of CO<sub>2</sub> was increased slightly when the volume of TEA was increased from 4% to 6%. This indicates that the consumption of TEA in the

dispersed aqueous phase of ELM increase sharply to 4% TEA, but above this, the absorption behavior of the ELM in RDC is in the slow regime.

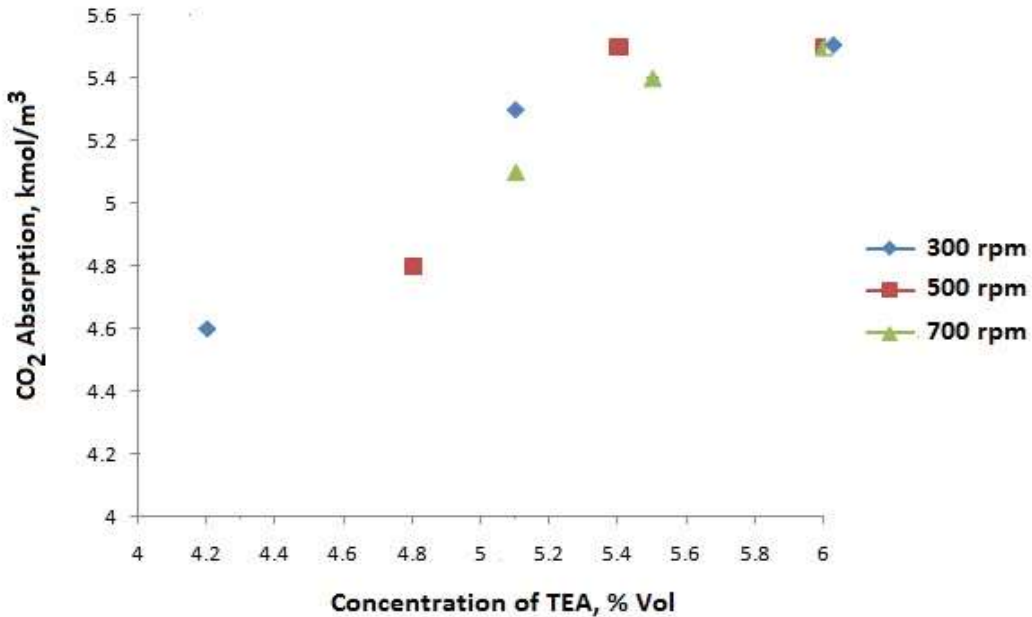


Figure 16. Effect of the TEA concentration on CO<sub>2</sub> absorption in the RDC for 30 min

Up to 4% TEA the RDC system was effective in absorbing the maximum amount of CO<sub>2</sub> from the CO<sub>2</sub>/CH<sub>4</sub> gas mixture. This study also determined that a higher concentration of absorbent in the dispersed aqueous phase of ELM will increase the concentration of CO<sub>2</sub> due to the high absorption of CO<sub>2</sub> from the CO<sub>2</sub>/CH<sub>4</sub> gas mixture. In earlier work by Rubia and García-Abuín [67], it was reported that the concentration of TEA has a linear influence on the CO<sub>2</sub> absorption in the gas-liquid interface of the bubble size. The study by Donaldson and Nguyen [68] on the

chemical reaction kinetics of CO<sub>2</sub> with TEA in the gas-liquid contact system found that the reaction rate increased with increasing TEA concentration.

## **7. Conclusion**

This paper outlined a simple and innovative method to prepare a stable ELM using the high-speed homogenization, which achieved high throughput at low power consumption. During ELM preparation, the emulsification speed and time influences the emulsion droplet size while the stability of the emulsion depends on the emulsion droplet size, concentration of constituents and pH.

Different surfactants were assessed to increase the stability of the ELM. The ELM containing 2% v/v of TEA could absorb 5.6 kmol/m<sup>3</sup> CO<sub>2</sub> at 500 rpm of RDC for 30 minutes operation. Based on the results related to the different speeds of RDC, the amount of absorbed CO<sub>2</sub> increased with increasing TEA concentration in the dispersed aqueous phase of ELM. In addition, at up to 4% TEA in the dispersed aqueous phase of ELM, the RDC system is effective in absorbing the maximum amount of CO<sub>2</sub> from the CO<sub>2</sub>/CH<sub>4</sub> gas mixture. This study also suggests that increasing the retention time of ELM in RDC also increases the amount of CO<sub>2</sub> absorbed. The performance of CO<sub>2</sub> absorption was enhanced by introducing an amine as a dispersed aqueous phase of the ELM in the RDC system. The ELM provides a large surface area by generating micrometer size particles. An increase in surface area enhances the mass transfer rate of the process. In addition, encapsulating the amine solution in ELM reduces its corrosiveness, thereby providing protection for the piping system.

Further studies will be needed to evaluate desorption of CO<sub>2</sub> from the proposed emulsion. In addition, hydrodynamic studies are also suggested to evaluate the performance of the modified design dimensions of the RDC.

## 8. Acknowledgement

The Study was funded by the Ministry of Science Technology and Innovation, Malaysia.

Experimental work was carried out at Chemical Engineering Department, Universiti Teknologi Malaysia.

## 9. References

1. Hwang, C.-C., et al., *Capturing carbon dioxide as a polymer from natural gas*. Nat Commun, 2014. **5**.
2. Kumar, S., J.H. Cho, and I. Moon, *Ionic liquid-amine blends and CO<sub>2</sub>BOLs: Prospective solvents for natural gas sweetening and CO<sub>2</sub> capture technology—A review*. International Journal of Greenhouse Gas Control, 2014. **20**(0): p. 87-116.
3. Lock, S.S.M., et al., *Modeling, simulation and economic analysis of CO<sub>2</sub> capture from natural gas using cocurrent, countercurrent and radial crossflow hollow fiber membrane*. International Journal of Greenhouse Gas Control, 2015. **36**: p. 114-134.
4. Rochelle, G.T., *Amine Scrubbing for CO<sub>2</sub> Capture*. Science, 2009. **325**(5948): p. 1652-1654.
5. Baker, R.W. and K. Lokhandwala, *Natural Gas Processing with Membranes: An Overview*. Industrial & Engineering Chemistry Research, 2008. **47**(7): p. 2109-2121.
6. Kulkarni, P.S. and V.V. Mahajani, *Application of liquid emulsion membrane (LEM) process for enrichment of molybdenum from aqueous solutions*. Journal of Membrane Science, 2002. **201**(1–2): p. 123-135.
7. Rabiee, H., A. Ghadimi, and T. Mohammadi, *Gas transport properties of reverse-selective poly(ether-b-amide6)/[Emim][BF<sub>4</sub>] gel membranes for CO<sub>2</sub>/light gases separation*. Journal of Membrane Science, 2015. **476**(0): p. 286-302.
8. Ahmad, F., et al., *Hollow fiber membrane model for gas separation: Process simulation, experimental validation and module characteristics study*. Journal of Industrial and Engineering Chemistry, 2015. **21**: p. 1246-1257.
9. Adewole, J.K., et al., *Current challenges in membrane separation of CO<sub>2</sub> from natural gas: A review*. International Journal of Greenhouse Gas Control, 2013. **17**(0): p. 46-65.
10. Li, N.N., *Separation of Hydrocarbons by Liquid Membrane Permeation*. Industrial & Engineering Chemistry Process Design and Development, 1971. **10**(2): p. 215-221.
11. Gameiro, M.L.F., et al., *Extraction of copper from ammoniacal medium by emulsion liquid membranes using LIX 54*. Journal of Membrane Science, 2007. **293**(1–2): p. 151-160.
12. Krull, F., C. Fritzmann, and T. Melin, *Liquid membranes for gas/vapor separations*. Journal of Membrane Science, 2008. **325**(2): p. 509-519.

13. Park, H.B., et al., *Relationship between chemical structure of aromatic polyimides and gas permeation properties of their carbon molecular sieve membranes*. Journal of Membrane Science, 2004. **229**(1-2): p. 117-127.
14. Linek, V. and P. Benes, *A Study of the Mechanism of Gas Absorption into Oil-Water Emulsions*. Chemical Engineering Science, 1976. **31**: p. 1037-1046.
15. Leal-Calderon, F., et al., *Water-in-Oil Emulsions: Role of the Solvent Molecular Size on Droplet Interactions*. Langmuir, 1997. **13**(26): p. 7008-7011.
16. Kamiński, W. and W. Kwapiński, *Applicability of Liquid Membranes in Environmental Protection*. Polish Journal of Environmental Studies 2000. **9**(1): p. 37-43.
17. Torab-Mostaedi, M. and M. Asadollahzadeh, *Mass transfer performance in an asymmetric rotating disc contactor*. Chemical Engineering Research and Design, 2015. **94**: p. 90-97.
18. Morís, M.A., F.V. Díez, and J. Coca, *Hydrodynamics of a rotating disc contactor*. Separation and Purification Technology, 1997. **11**(2): p. 79-92.
19. Vasiljevic, D., G. Vuleta, and M. Primorac, *The characterization of the semi-solid W/O/W emulsions with low concentrations of the primary polymeric emulsifier*. International Journal of Cosmetic Science, 2005. **27**(2): p. 81-87.
20. Vasiljevic, D., G. Vuleta, and M. Primorac, *The characterization of the semi-solid W/O/W emulsions with low concentration of the primary polymeric emulsifier*. International Journal of Cosmetic Science, 2005. **27**: p. 81-87.
21. Hanna, G.J. and K.M. Larson, *Influence of preparation parameters on internal droplet size distribution of emulsion liquid membranes*. Industrial & Engineering Chemistry Product Research and Development, 1985. **24**(2): p. 269-274.
22. Vecht-Lifshitz, S.E. and A.P. Ison, *Biotechnological applications of image analysis: present and future prospects*. Journal of Biotechnology, 1992. **23**(1): p. 1-18.
23. Walstra, P., *Principles of emulsion formation*. Chemical Engineering Science, 1993. **48**(2): p. 333-349.
24. Tcholakova, S., et al., *Interrelation between Drop Size and Protein Adsorption at Various Emulsification Conditions*. Langmuir, 2003. **19**(14): p. 5640-5649.
25. Pons, R., et al., *Formation and properties of miniemulsions formed by microemulsions dilution*. Advances in Colloid and Interface Science, 2003. **106**(1-3): p. 129-146.
26. Mabile, C., et al., *Monodisperse fragmentation in emulsions: Mechanisms and kinetics*. Europhysics Letters, 2003. **61**(05): p. 708-714.
27. Djaković, L., et al., *Action of emulsifiers during homogenization of o/w emulsions*. Colloid & Polymer Science, 1987. **265**(11): p. 993-1000.
28. Sánchez, M.C., et al., *Emulsification Rheokinetics of Nonionic Surfactant-Stabilized Oil-in-Water Emulsions*. Langmuir, 2001. **17**(18): p. 5410-5416.
29. Oh, S.G., M. Jobalia, and D.O. Shah, *The Effect of Micellar Lifetime on the Droplet Size in Emulsions*. Journal of Colloid and Interface Science, 1993. **156**(2): p. 511-514.
30. Tornberg, E., *Functional characterization of protein stabilized emulsions: Emulsifying behaviour of proteins in a valve homogenizer*. Journal of the Science of Food and Agriculture, 1978. **29**(10): p. 867-879.
31. Tornberg, E., *Functional Characteristics of Protein Stabilized Emulsions: Emulsifying Behavior of Proteins in a Sonifier*. Journal of Food Science, 1980. **45**(6): p. 1662-1668.
32. Maa, Y.-F. and C. Hsu, *Liquid-liquid emulsification by rotor/stator homogenization*. Journal of Controlled Release, 1996. **38**(2-3): p. 219-228.

33. Raikar, N.B., et al., *Predicting the Effect of the Homogenization Pressure on Emulsion Drop-Size Distributions*. Industrial & Engineering Chemistry Research, 2011. **50**(10): p. 6089-6100.
34. Venkatesan, S. and K.M.M.S. Begum, *Removal of copper and zinc from aqueous solutions and industrial effluents using emulsion liquid membrane technique*. Asia-Pacific Journal of Chemical Engineering, 2008. **3**(4): p. 387-399.
35. Leong, T.S.H., et al., *Minimising oil droplet size using ultrasonic emulsification*. Ultrasonics Sonochemistry, 2009. **16**(6): p. 721-727.
36. Israelachvili, J., *The science and applications of emulsions - an overview*. Colloids and Surfaces A: Physicochemical and Engineering Aspects, 1994. **91**(C): p. 1-8.
37. Oh, D.H., et al., *Effect of process parameters on nanoemulsion droplet size and distribution in SPG membrane emulsification*. International Journal of Pharmaceutics, 2011. **404**(1-2): p. 191-197.
38. Tadros, T., et al., *Formation and stability of nano-emulsions*. Advances in Colloid and Interface Science, 2004. **108-109**: p. 303-318.
39. Opawale, F.O. and D.J. Burgess, *Influence of Interfacial Rheological Properties of Mixed Emulsifier Films on the Stability of Water-in-Oil-in-Water Emulsions*. Journal of Pharmacy and Pharmacology, 1998. **50**(9): p. 965-973.
40. Derkach, S.R., *Rheology of emulsions*. Advances in Colloid and Interface Science, 2009. **151**(1-2): p. 1-23.
41. Fischer, P. and P. Erni, *Emulsion drops in external flow fields — The role of liquid interfaces*. Current Opinion in Colloid & Interface Science, 2007. **12**(4-5): p. 196-205.
42. Stevens, G.W., J.M. Perera, and F. Grieser, *Metal ion extraction*. Current Opinion in Colloid & Interface Science, 1997. **2**(6): p. 629-634.
43. Stevens, G.W., *Interfacial Phenomena in Solvent Extraction and Its Influence on Process Performance*. Tsinghua Science & Technology, 2006. **11**(2): p. 165-170.
44. Broughton, G. and L. Squires, *The Viscosity of Oil-Water Emulsions*. Journal of Physical Chemistry, 1938. **42**(2): p. 253-263.
45. Pandolfe, W.D., *Effect of dispersed and continuous phase viscosity on droplet size of emulsions generated by homogenization*. Journal of Dispersion Science and Technology, 1981. **2**(4): p. 459 - 474.
46. Liu, W., et al., *Formation and stability of paraffin oil-in-water nano-emulsions prepared by the emulsion inversion point method*. Journal of Colloid and Interface Science, 2006. **303**(2): p. 557-563.
47. Boyacı, F.G., S. Takaç, and T.H. Özdamar, *Catalytic effect of NaOH on the liquid-phase oxidation of 2-isopropyl-naphthalene*. Applied Catalysis A: General, 1998. **172**(1): p. 59-66.
48. Schwarz, H.A., *Chain decomposition of aqueous triethanolamine*. The Journal of Physical Chemistry, 1982. **86**(17): p. 3431-3435.
49. Yang, F., et al., *Effect of dispersion pH on the formation and stability of Pickering emulsions stabilized by layered double hydroxides particles*. Journal of Colloid and Interface Science, 2007. **306**(2): p. 285-295.
50. Stachurski, J. and M. Michalek, *The effect of the  $\zeta$  potential on the stability of a non-polar oil-in-water emulsion*. Journal of Colloid and Interface Science, 1996. **184**(2): p. 433-436.
51. Ren, Z., et al., *Modeling of Effect of pH on Mass Transfer of Copper(II) Extraction by Hollow Fiber Renewal Liquid Membrane*. Industrial & Engineering Chemistry Research, 2008. **47**(12): p. 4256-4262.

52. Katsuroku, T., O. Fujio, and T. Hiroshi, *A Study of the Stability of (w/o)/w-Type Emulsions Using a Tracer Technique*. Journal of Chemical Engineering of Japan, 1981. **14**(5): p. 416-418.
53. Soottitantawat, A., et al., *Influence of emulsion and powder size on the stability of encapsulated D-Limonene by spray drying*. Innovative Food Science and Emerging Technologies, 2005. **6**: p. 107-114.
54. Ventureira, J., E.N. Martínez, and M.C. Añón, *Stability of oil: Water emulsions of amaranth proteins. Effect of hydrolysis and pH*. Food Hydrocolloids, 2010. **24**(6-7): p. 551-559.
55. Barad, J.M., M. Chakraborty, and H.-J.r. Bart, *Stability and Performance Study of Water-in-Oil-in-Water Emulsion: Extraction of Aromatic Amines*. Industrial & Engineering Chemistry Research, 2010. **49**(12): p. 5808-5815.
56. Fontenot, K. and F.J. Schork, *Sensitivities of droplet size and stability in monomeric emulsions*. Industrial & Engineering Chemistry Research, 1993. **32**(2): p. 373-385.
57. Matsumoto, S., *Formation and Stability of Water-in-Oil-in-Water Emulsions*, in *Macro- and Microemulsions*. 1985, American Chemical Society. p. 415-436.
58. Kamarudin, K.S.N., et al., *Removal of Carbon Dioxide Using Water-in-Oil Emulsion Liquid Membrane Containing Triethanolamine*. Journal of Applied Sciences Research, 2010. **6**(12): p. 2251-2256.
59. Boyd, J., C. Parkinson, and P. Sherman, *Factors affecting emulsion stability, and the HLB concept*. Journal of Colloid and Interface Science, 1972. **41**(2): p. 359-370.
60. Takahshi, K., S. Nii, and F. Kawaizumi, *Absorption Rate of Carbon Dioxide by K<sub>2</sub>CO<sub>3</sub>-KHCO<sub>3</sub> DEA Aqueous Solution*. Developments in Chemical Engineering and Mineral Processing, 2005. **13**(1-2): p. 159-176.
61. Park, S.W., B.S. Choi, and J.W. Lee, *Chemical absorption of carbon dioxide into aqueous elastic xanthan gum solution containing NaOH*. Journal of Industrial and Engineering Chemistry, 2008. **14**(3): p. 303-307.
62. Park, S.W., et al., *Chemical absorption of carbon dioxide with NaOH in non-Newtonian w/o emulsion*, in *Studies in Surface Science and Catalysis*, E.P. Sang, J.S. Chang, and L. Kyu Wan, Editors. 2004, Elsevier. p. 523-526.
63. Lin, C.-C. and B.-C. Chen, *Carbon Dioxide Absorption into NaOH Solution in a Cross-flow Rotating Packed Bed*. Journal of Industrial Engineering Chemistry, 2007. **13**(7): p. 1083-1090.
64. Tedajo, G.M., et al., *pH compartmented w/o/w multiple emulsion: a diffusion study*. Journal of Controlled Release, 2001. **75**(1-2): p. 45-53.
65. Hagewiesche, D.P., et al., *Absorption of carbon dioxide into aqueous blends of monoethanolamine and N-methyldiethanolamine*. Chemical Engineering Science, 1995. **50**(7): p. 1071-1079.
66. Brogren, C. and H.T. Karlsson, *Modeling the absorption of SO<sub>2</sub> in a spray scrubber using the penetration theory*. Chemical Engineering Science, 1997. **52**(18): p. 3085-3099.
67. Rubia, M.D.L., et al., *Interfacial area and mass transfer in carbon dioxide absorption in TEA aqueous solutions in a bubble column reactor*. Chemical Engineering and Processing: Process Intensification, 2010. **49**(8): p. 852-858.
68. Donaldson, T.L. and Y.N. Nguyen, *Carbon Dioxide Reaction Kinetics and Transport in Aqueous Amine Membranes*. Industrial & Engineering Chemistry Fundamentals, 1980. **19**(3): p. 260-266.